Do Reuss and Voigt bounds really bound in high-pressure rheology experiments?

2006 J. Phys.: Condens. Matter 18 S1049

(http://iopscience.iop.org/0953-8984/18/25/S11)

INSTITUTE OF PHYSICS PUBLISHING JOURNAL OF PHYSICS: CONDENSED MATTER

J. Phys.: Condens. Matter **18** (2006) S1049–S1059 doi:10.1088/0953-8984/18/25/S11

Do Reuss and Voigt bounds really bound in high-pressure rheology experiments?

Jiuhua Chen, Li Li, Tony Yu, Hongbo Long, Donald Weidner, Liping Wang and Michael Vaughan

Mineral Physics Institute and Department of Geosciences, Stony Brook University, Stony Brook, NY 11794-2100, USA

E-mail: Jiuhua.Chen@sunysb.edu

Received 17 February 2006, in final form 4 May 2006
Published 8 June 2006
Online at stacks.iop.org/JPhysCM/18/S1049

Abstract

Energy dispersive synchrotron x-ray diffraction is carried out to measure differential lattice strains in polycrystalline Fe_2SiO_4 (fayalite) and MgO samples using a multi-element solid state detector during high-pressure deformation. The theory of elastic modelling with Reuss (iso-stress) and Voigt (iso-strain) bounds is used to evaluate the aggregate stress and weight parameter, α ($0 \leqslant \alpha \leqslant 1$), of the two bounds. Results under the elastic assumption quantitatively demonstrate that a highly stressed sample in high-pressure experiments reasonably approximates to an iso-stress state. However, when the sample is plastically deformed, the Reuss and Voigt bounds are no longer valid (α becomes beyond 1). Instead, if plastic slip systems of the sample are known (e.g. in the case of MgO), the aggregate property can be modelled using a visco-plastic self-consistent theory.

1. Introduction

In situ x-ray diffraction plays a central role in modern high-pressure deformation experiments for deriving external stress applied to an aggregate sample in a high-pressure cell (Merkel *et al* 2002, Wang *et al* 2003, Chen *et al* 2004, Li *et al* 2004, Weidner *et al* 2004, Nishiyama *et al* 2005). In a traditional high-pressure deformation experiment, the sample stress and strain are determined by measuring the force and the displacement of a piston that extends from the sample to outside of the high-pressure cell (Tingle *et al* 1993). Exploiting synchrotron x-rays makes the stress and strain measurements possible without the piston in a conventional deformation apparatus (i.e. Paterson Press), and therefore significantly advances the maximum pressure range for deformation experiments.

Rheology at high pressures is a critical property of minerals in governing the process of mantle dynamics. For understanding the process of mantle convection, the origin of deep earthquakes, and the cause of seismic anisotropy, knowledge of the rheological properties of

minerals at mantle pressures is essential (Karato and Wu 1993). Developments of *in situ* x-ray diffraction at synchrotron facilities have greatly advanced the pressure range for deformation experiments (Weidner *et al* 1998, Wang *et al* 2003). Whereas many plastic behaviours (e.g. texture, active slip system) of minerals can be investigated without direct strain/stress measurements, deriving flow laws (the most fundamental rheological property) requires quantifying the strain and stress applied to the sample at high pressures. In the deformation experiments in conjunction with high penetration power synchrotron x-rays, the sample strain can be measured through x-ray radiograph imaging and the sample stress can be derived by measuring the variation in lattice strain of a polycrystalline sample as a function of the orientation with respect to the differential stress field (Chen *et al* 2004, Li *et al* 2004, Nishiyama *et al* 2005). The orientation dependence of the lattice strain can be measured through either two-dimensional x-ray diffraction using a monochromatic beam or multiple energy-dispersive x-ray diffractions using a white beam. However, the x-ray diffraction actually infers the elastic lattice strains of the particular population of grains orientated along the diffraction vector. To derive the stress externally applied to the bulk aggregate sample, one needs to model the stress/strain propagation through the grain-to-grain contact in the bulk sample. A conventional method of modelling is to use elastic Reuss and Voigt bounds (Singh 1993, Funamori *et al* 1994, Uchida *et al* 1996, Singh *et al* 1998, Chen *et al* 2004). The Reuss bound describes an extreme condition (iso-stress) under which all the grains in the bulk sample experience identical stress when forces are applied to the sample (Reuss 1929), while the Voigt bound describes another extreme, that all the grains experience the same strain when the bulk sample is deformed under stress (Voigt 1928). An intermediate condition is then described by combining the bounds with a weight parameter α ($0 \leqslant \alpha \leqslant 1$; $\alpha = 1$ and 0 represent the Reuss and Voigt conditions respectively).

Modelling the stress field under this principle has been commonly adopted to derive the applied stress, strength, elastic anisotropy, and even elastic constants of materials under high pressures in a diamond anvil cell (DAC) (Singh 1993, Mao *et al* 1998, Singh *et al* 1998, Kavner and Duffy 2001, Merkel *et al* 2002, Kavner 2003, Shieh *et al* 2004) or a multi-anvil press (MAP) (Wang *et al* 2003, Chen *et al* 2004, Li *et al* 2004, Weidner *et al* 2004, Nishiyama *et al* 2005). In recent DAC studies, (Kavner and Duffy 2001, Kavner 2003) realized that the elastic anisotropy of a ringwoodite sample derived from the above method is significantly lower than that measured through the Brillouin scattering technique (Sinogeikin *et al* 2003). An x-ray diffraction study on MgO by Merkel *et al* (2002) also indicates a low elastic anisotropy with respect to the result from Brillouin scattering (Sinogeikin and Bass 1999) in the pressure range 6–20 GPa. These discrepancies are interpreted as a result of stress redistribution due to plastic flow in the sample (Weidner *et al* 2004).

In this paper, we report the evolution of the weight parameter α of an Fe_2SiO_4 (fayalite) sample during plastic flow/deformation at high pressures, measured in a MAP using x-ray diffraction. The result indicates that once large plastic flow occurs, the elastic model using Reuss and Voigt bounds cannot be applied to the system—the α value goes beyond the boundary condition ($0 \leqslant \alpha \leqslant 1$). On the other hand, experimental data obtained from an MgO sample demonstrate that in the plastic regime a slip system governed visco-plastic self-consistent model is more appropriate to describe the stress/strain propagation in an aggregate sample.

2. Deriving the weight parameter α for Reuss and Voigt bounds

The deformation sample in a MAP is often considered under an approximate cylindrical stress field (figure 1) with $\sigma 1 = \sigma 2 \neq \sigma 3$ and

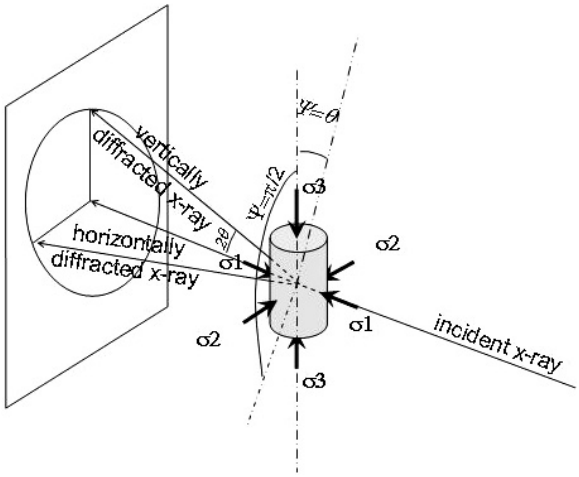

Figure 1. Geometric sketch of the relation between the x-ray diffraction vector and stress fields in a multi-anvil high-pressure apparatus. θ: Bragg angle of the x-ray diffraction, ψ: the angle between the diffraction vector and the principal stress ($\sigma 3$) axis.

$$\sigma_{ij} = \begin{pmatrix} \sigma 1 & 0 & 0 \\ 0 & \sigma 1 & 0 \\ 0 & 0 & \sigma 3 \end{pmatrix} = \begin{pmatrix} \sigma_{\mathrm{P}} & 0 & 0 \\ 0 & \sigma_{\mathrm{P}} & 0 \\ 0 & 0 & \sigma_{\mathrm{P}} \end{pmatrix} + \begin{pmatrix} -t/3 & 0 & 0 \\ 0 & -t/3 & 0 \\ 0 & 0 & 2t/3 \end{pmatrix} \tag{1}$$

where $\sigma 1$ and $\sigma 3$ are radial and axial stress components, respectively; σ_{p} is the mean normal stress (hydrostatic pressure); t is the differential stress. As each individual peak (hkl) in a given diffraction pattern represents the elastic strain of a grain subpopulation which has the (hkl) lattice orientated along the diffraction vector (a direction bisecting the angle between incident and diffracted beams), the observed peak position (d-spacing) varies with the orientation of the diffraction vector relative to the stress field applied to the sample (i.e. ψ angle in figure 1). The relation between the measured lattice strain and the ψ angle can be described as (Singh *et al* 1998)

$$\varepsilon(hkl) = \varepsilon_{\mathrm{P}} + \tfrac{1}{3}t(1 - 3\cos^2\psi)\left\{\alpha[2G_{\mathrm{R}}(hkl)]^{-1} + (1-\alpha)(2G_{\mathrm{V}})^{-1}\right\} \tag{2}$$

where ε_{P} is strain component due to the hydrostatic pressure in the total stress; $G_{\mathrm{R}}(hkl)$ is the aggregate shear modulus calculated under the Reuss condition; G_{V} is the shear modulus under the Voigt condition. If we let ε_{H} and ε_{V} represent the lattice strain measured at $\psi = \pi/2$ and $\psi = 0$, then

$$\varepsilon_{\mathrm{H}}(hkl) = \varepsilon_{\mathrm{P}} + \tfrac{1}{3}t\left\{\alpha[2G_{\mathrm{R}}(hkl)]^{-1} + (1-\alpha)(2G_{\mathrm{V}})^{-1}\right\}$$
$$\varepsilon_{\mathrm{V}}(hkl) = \varepsilon_{\mathrm{P}} - \tfrac{2}{3}t\left\{\alpha[2G_{\mathrm{R}}(hkl)]^{-1} + (1-\alpha)(2G_{\mathrm{V}})^{-1}\right\}$$

Therefore,

$$\begin{aligned}\Delta\varepsilon(hkl) &\equiv \varepsilon_{\mathrm{H}}(hkl) - \varepsilon_{\mathrm{V}}(hkl) \\ &= t\alpha[2G_{\mathrm{R}}(hkl)]^{-1} + t(1-\alpha)(2G_{\mathrm{V}})^{-1}.\end{aligned} \tag{3}$$

The weight parameter α can then be derived by plotting the observed $\Delta\varepsilon(hkl)$ for each diffraction peak (hkl) as a function of $[2G_{\mathrm{R}}(hkl)]^{-1}$:

$$\alpha = \frac{a}{a + 2bG_{\mathrm{V}}} \tag{4}$$

where a and b are the slope and the intercept on the $\Delta\varepsilon(hkl)$ axis of the plot, respectively.

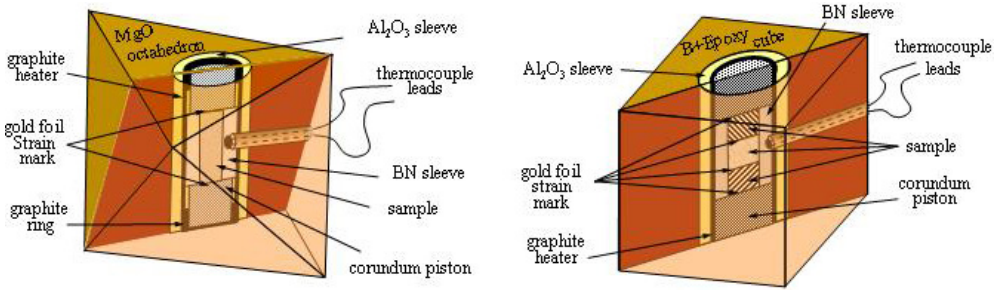

Figure 2. Cell assemblies used for deformation experiments. (a) Octahedral pressure medium with 8 mm edge-length for T-cup apparatus; (b) cubic pressure medium with 6 mm edge-length for D-DIA apparatus. Dense corundum pistons are used on both ends of the sample for delivering differential stress to the specimen.

(This figure is in colour only in the electronic version)

Expressions for $[2G_R(hkl)]^{-1}$ for different crystal systems can be found in Singh *et al* (1998).

Cubic system:

$$[2G_R(hkl)]^{-1} = [S_{11} - S_{12} - 3(S_{11} - S_{12} - 1/2S_{44})](h^2k^2 + k^2l^2 + l^2h^2)/(h^2 + k^2 + l^2)^2 \tag{5}$$

Orthorhombic system:

$$\begin{aligned}[2G_R(hkl)]^{-1} = 1/2\{&-(S_{12} + S_{13} + S_{23}) + l_1^2(S_{23} - S_{11}) + l_2^2(S_{13} - S_{22}) + l_3^2(S_{12} - S_{33}) \\ &+ 3[l_1^4S_{11} + l_2^4S_{22} + l_3^4S_{33} + l_1^2l_2^2(2S_{12} + S_{66}) + l_2^2l_3^2(2S_{23} + S_{44}) \\ &+ l_3^2l_1^2(2S_{13} + S_{55})]\}\end{aligned} \tag{6}$$

where $l_1 = hd(hkl)/a$, $l_2 = kd(hkl)/b$, and $l_3 = ld(hkl)/c$; $d(hkl)$: spacing between (hkl) lattice planes. a, b, and c: the unit cell dimensions; S_{ij}: elastic compliance.

Expressions for G_V for different crystal systems can be found in Hearmon (1956).

Cubic system:

$$G_V = 1/5(C_{11} - C_{12} + 3C_{44}) \tag{7}$$

Orthorhombic system:

$$G_V = 1/15(C_{11} + C_{22} + C_{33} - C_{12} - C_{23} - C_{31} + 3C_{44} + 3C_{55} + 3C_{66}) \tag{8}$$

where C_{ij} are elastic stiffnesses.

3. The experiments and results

Experiments were conducted on polycrystalline Fe_2SiO_4 and MgO specimens to investigate the evolution of the weight parameter during plastic flow. The experiment on the Fe_2SiO_4 sample was carried out using a 6–8 double-stage multi-anvil press, T-cup (a compact tea-cup size multi-anvil apparatus, Vaughan *et al* 1998); x-ray diffractions were recorded during the plastic flow induced by thermal relaxation in the sample at high pressure. The experiments on the MgO sample were performed using a deformation DIA (D-DIA) apparatus (a cubic-type multi-anvil press with add-on differential rams for driving top and bottom anvils independently, Wang *et al* 2003); plastic deformation was introduced by advancing the differential rams of the D-DIA at high pressure. The cell assemblies used in the experiments are shown in

Table 1. Elastic constants of Fe_2SiO_4 used in the calculation (Graham *et al* 1988).

	$P = 0$ GPa, $T = 300$ K	$\partial C_{ij}/\partial T$ (GPa K^{-1})	$\partial C_{ij}/\partial P$
C_{11}	265.85	−0.052	7.37
C_{22}	160.25	−0.0524	5.29
C_{33}	222.42	0.0378	5.2
C_{12}	92.4	−0.027	6.08
C_{13}	80.6	−0.015	5.7
C_{23}	88.4	−0.012	3.5
C_{44}	31.55	−0.0098	2.49
C_{55}	46.74	−0.0096	1.35
C_{66}	57.15	−0.0175	1.7

Table 2. Elastic constants of MgO used in the calculation (Spetzler 1970).

	$P = 0$ GPa, $T = 300$ K	$\partial C_{ij}/\partial T$ (GPa K^{-1})	$\partial C_{ij}/\partial P$
C_{11}	297.4	−0.0613	8.68
C_{12}	95.6	0.0044	1.38
C_{44}	156.2	−0.0116	1.14

figure 2. Configurations of 8 mm edge-length octahedral pressure medium (MgO) versus 2 mm second-stage anvil (cBN and WC) truncation and 6 mm edge-length cubic pressure medium (mixture of boron and epoxy resin, 4:1) versus 4 mm DIA anvil truncation were used in the T-cup and D-DIA experiments, respectively. The sample temperature was measured using a W–3% Re/W–25% Re thermocouple (no correction was made for pressure dependence of the EMF—electromotive force). The sample pressure was derived based on the sample elastic constants and their pressure/temperature dependence (table 1 and table 2) from published literatures (Spetzler 1970, Graham *et al* 1988). Energy dispersive x-ray diffraction patterns were collected using a 13-element Ge solid state detector. A conic slit was used to collimate the diffracted x-ray from the sample in such a way that 4 of the 13 elements of the detector record diffraction patterns at 2θ angles of $\sim\pm 6.5^\circ$ in the vertical and horizontal diffraction planes simultaneously. An x-ray radiography system was used to record the change in sample length. Details of the *in situ* stress and strain measurement system of the multi-anvil high-pressure station at the X17B beamline of the National Synchrotron Light Source (NSLS) can be found elsewhere (Chen *et al* 2004).

A powdered Fe_2SiO_4 sample (fayalite, orthorhombic structure, space group: $Pbnm$, synthesized at Stony Brook University) with an average grain size of ~ 1 μm was packed into a cylindrical sample chamber of 1 mm diameter and about 3 mm in length.

The sample was first compressed at room temperature and then annealed at 973 K. After being quenched to room temperature, the sample was further compressed. Large differential stress was built up along the cylindrical axis during the compression because of the hard pistons (no other soft buffering material in series) at each end of the sample. Upon heating to 773 K, plastic flow (shortening) of the sample under this differential stress occurred. No shortening was observed in the hard pistons. X-ray diffraction patterns from the sample were recorded during the plastic flow. Figure 3 shows two diffraction patterns recorded simultaneously in horizontal and vertical diffraction planes, $\psi = 90^\circ$ and θ ($2\theta = 6.5^\circ$). The value of $\varepsilon_V(hkl)$ ($\psi = 0$) is then derived using (Chen *et al* 2004)

$$\varepsilon_V(hkl) = \frac{\varepsilon_{\psi=\theta}(hkl) - \varepsilon_H(hkl)\sin^2\theta}{\cos^2\theta}. \tag{9}$$

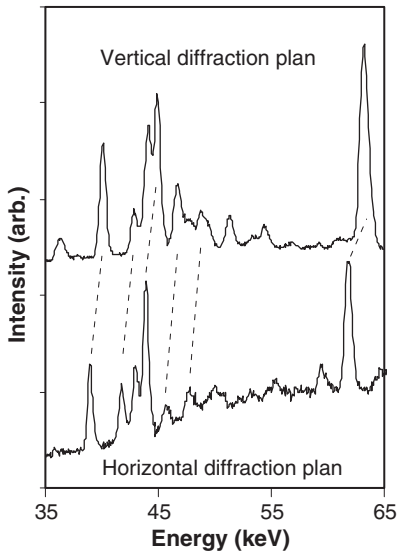

Figure 3. Diffraction patterns of the Fe_2SiO_4 sample at 4.5 GPa and 773 K, collected simultaneously on the detector allocated in the vertical and horizontal diffraction planes ($2\theta = 6.5°$). Differential stress applied to the sample (figure 1) results in the relative shift of diffraction peaks in the patterns collected at different ψ angles.

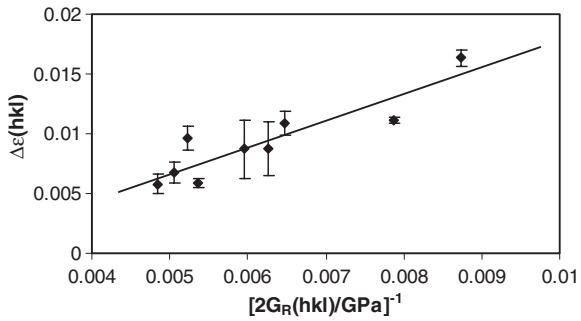

Figure 4. Differential elastic lattice strain $\Delta\varepsilon(hkl) = \varepsilon_H(hkl) - \varepsilon_V(hkl)$ versus Reuss aggregate shear modulus $[2G_R(hkl)]^{-1}$ of Fe_2SiO_4 at 4.5 GPa 773 K. Bars attached to symbols represent experimental errors. The solid line is a linear fit of the experimental data, from which the weight parameter α for Reuss and Voigt bounds is derived (see text).

Figure 4 shows a typical plot of $\Delta\varepsilon(hkl)$ versus $[2G_R(hkl)]^{-1}$ for deriving the weight parameter α using equation (4). The derived weight parameter α and the differential stress held by the specimen during the relaxation process are shown in figure 5 as a function of time of heating.

For the two MgO experiments, the powdered MgO sample was sandwiched between two single crystals (MgO{111} and MgO{100}) in the first run (as shown in figure 2, top sample: MgO{111}, middle: MgO powder, bottom: MgO{100}), and loaded with a Ta rod in series along the deformation axis in the second (as shown in figure 2, both the top and middle samples are MgO powder, and the bottom is the Ta rod). The experiments were conducted by compressing the sample at room temperature and then annealing the sample at high pressure (the pressure was slightly different in the two experiments; see below). While

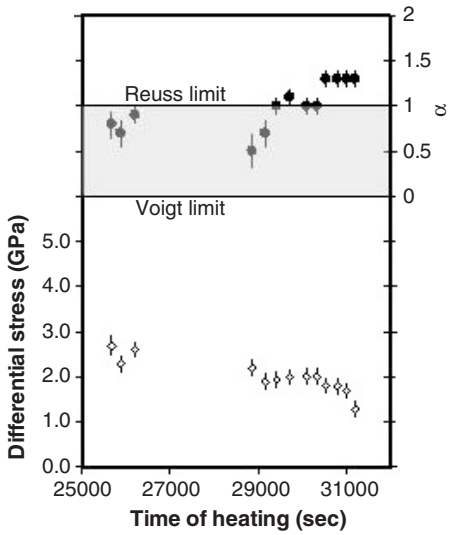

Figure 5. Evolution of the differential stress in the Fe_2SiO_4 sample and the weight parameter α for Reuss and Voigt bounds derived from x-ray diffraction during relaxation, as a function of time of heating (clock started at initial compression). Bars attached to symbols represent experimental errors. The shaded area indicates the elastic regime defined by Reuss and Voigt bounds.

maintaining the sample at high pressure and temperature, the top and bottom anvils of the D-DIA press were advanced, independently of the four side-anvils, to deform the sample. The sample length and diffraction pattern from the MgO powder were recorded.

In the first MgO experiment, both MgO{111} and MgO{100} single crystals exhibited significant plastic shortening during the deformation, whereas the polycrystalline MgO specimen showed no measurable plastic deformation. The elastic lattice strains $\Delta\varepsilon(200)$ and $\Delta\varepsilon(111)$ in the polycrystalline sample derived from x-ray diffractions at 5.7 GPa are plotted in figure 6 as a function of time. Shown in figure 6 is also the weight parameter α derived from these elastic lattice strains.

In the second experiment, the MgO sample length was notably shortened during the deformation. The elastic lattice strains $\Delta\varepsilon(200)$ and $\Delta\varepsilon(111)$ of the sample at 4.5 GPa, as well as the derived weight parameter α, are plotted in figure 7 as a function of time.

4. Discussion

The weight parameter α measured during the plastic flow of relaxation in the Fe_2SiO_4 experiment indicates a near Reuss bound (α close to 1) stress propagation in the largely stressed sample at the beginning (figure 5). However, as the plastic flow proceeds the weight parameter α increases, reaching the boundary defined by Reuss bound ($\alpha = 1$), and goes beyond the Reuss bound. This demonstrates that when plastic yielding takes place the stress distribution in the polycrystalline sample is no longer restrained by the elastic property of the material, and therefore the boundary defined by the elastic model does not bound in the plastic process. Deformation experiments on MgO specimens using the D-DIA, which generates plastic flow by advancing differential rams at a constant temperature, also reveal a result that is consistent with this conclusion. Lacking comprehensive understanding of slip systems in fayalite, the following discussion on modelling the differential stress during plastic flow only focuses on the case of MgO.

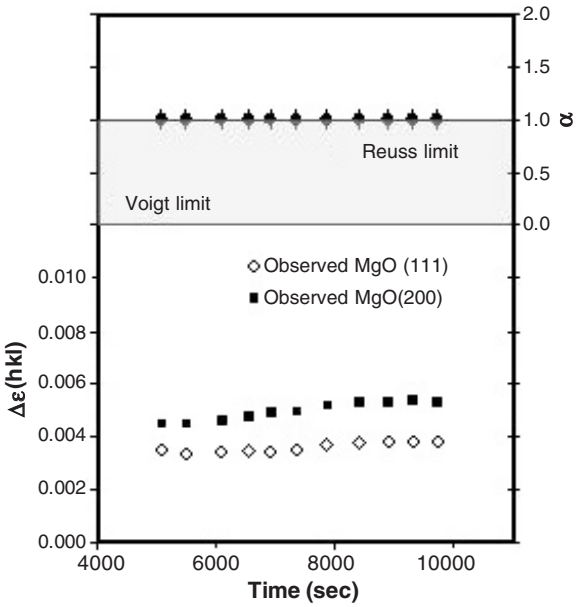

Figure 6. Differential elastic lattice strains $\Delta\varepsilon(200)$ and $\Delta\varepsilon(111)$ of polycrystalline MgO (bottom) and the derived weight parameter α for Reuss and Voigt bounds (top) at 5.7 GPa and 773 K when no notable plastic deformation in the aggregate is observed. Estimated experimental uncertainties are indicated by either the bars attached to symbols or the size of the symbols. The shaded area indicates the elastic regime defined by Reuss and Voigt bounds. The fact that $\alpha \approx 1$ indicates a near iso-stress state of the system at this condition.

Previous studies (Copley and Pask 1965a, 1965b, Paterson and Weaver 1970, Skrotzki and Welch 1983, Meade and Jeanloz 1988, Foitzik *et al* 1989, Stretton *et al* 2001, Wenk 2002, Yamazaki and Karato 2002) have suggested three soft slip systems in MgO crystal: $\{110\}\langle 1\bar{1}0\rangle$, $\{111\}\langle 1\bar{1}0\rangle$ and $\{100\}\langle 011\rangle$. In our MgO deformation experiment, the polycrystalline sample is sandwiched between {111} and {200} single crystals and therefore the large strain generated by the D-DIA differential ram on the sequential samples is compensated by plastic flow of the single crystals because of the soft slip systems. Consequently, the polycrystalline sample has a near elastic behaviour with the weight parameter α right on the Reuss boundary ($\alpha = 1$); see figure 6. Nevertheless, when the polycrystalline sample experiences plastic deformation (as the single crystal strain-compensator is replaced by a Ta rod) the weight parameter α goes beyond the Reuss boundary (figure 7). Note that when plastic flow occurs there is a significant change in the ratio of elastic lattice strains $\Delta\varepsilon(200)$ to $\Delta\varepsilon(111)$ in the polycrystalline MgO sample, from $\Delta\varepsilon(200) > \Delta\varepsilon(111)$ in figure 6 to $\Delta\varepsilon(200) < \Delta\varepsilon(111)$ in figure 7. This can give rise to a dramatic change of apparent elastic anisotropy if the same elastic modelling is applied to both cases, causing the discrepancies between the results from Brillouin scattering measurements (without plastic deformation) (Sinogeikin and Bass 1999) and x-ray diffractions (with plastic deformation) at high pressures (Merkel *et al* 2002).

Plasticity in polycrystalline aggregates has increasingly drawn attention in high-pressure x-ray studies. Early classic theories in modelling plastic deformation include the Taylor model (homogeneous plastic strain, independent to grain orientation) (Taylor 1938) and the Sachs model (homogeneous ratio of stress components among grains) (Sachs 1928). Similarly to the elastic case, these simple assumptions are not usually maintained in real materials.

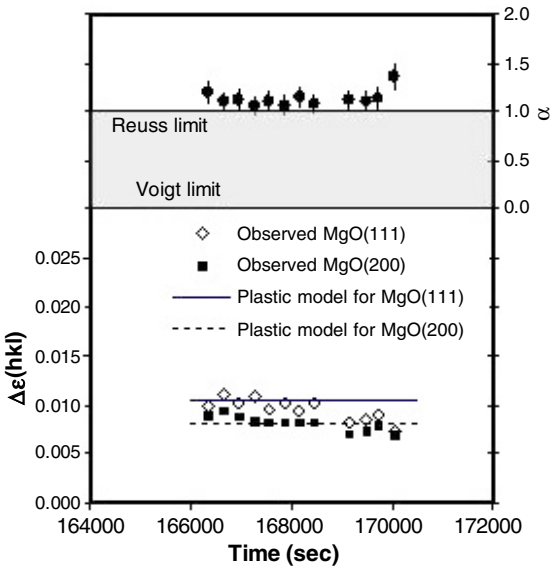

Figure 7. Differential elastic lattice strains $\Delta\varepsilon(200)$ and $\Delta\varepsilon(111)$ of polycrystalline MgO (bottom) and the derived weight parameter α for Reuss and Voigt bounds (top) at 4.5 GPa and 773 K when significant plastic deformation in the aggregate is observed. Estimated experimental uncertainties are indicated by either the bars attached to symbols or the size of the symbols. The shaded area indicates the elastic regime defined by Reuss and Voigt bounds. The ratio of $\Delta\varepsilon(200)/\Delta\varepsilon(111)$ changes from >1 in the elastic case (figure 6) to <1. The solid line and dotted line indicate scaled values for $\Delta\varepsilon(200)$ and $\Delta\varepsilon(111)$ based on the visco-plastic self-consistent modelling.

Extensions from these models have been made by for example Hill (1965), Berveiller and Zaoui (1981), Molinari *et al* (1987), and Lebensohn and Tome (1993) for incremental linearization, secant and tangent approach (also see a summary by Gilormini and Bréchet 1999). In recent years, a visco-plastic self-consistent (VPSC) model has been developed and widely applied to plastically deformed aggregates. This method averages the properties of polycrystal plasticity by considering each grain as an inclusion in a homogeneous medium and rigorously accounting for grain interactions directly. The VPSC model has become a very useful tool for analysing and simulating the deformation history from the observed texture, and it was successfully applied for modelling textures developed in minerals at high pressures (e.g. Wenk 1999, Merkel *et al* 2002). Very recently, Li *et al* (2004) demonstrated a sensible prediction of stress and elastic lattice strain distribution in MgO under uniaxial compression using the VPSC simulation model developed by (Clausen 1997, Clausen and Lorentzen 1997). This model assumes slip being the dominant deformation mechanism and other mechanisms being negligible. Slip occurs when the shear stress on the slip plane, and in the slip direction, reaches a value τ_{CRSS}, the critical resolved shear stress. All active slip systems contribute to the overall strain and stress of the aggregate with a weight of their own CRSS (critical resolved shear stress) ratio. Using this model and assuming three active slip systems in MgO (i.e. $\{110\}\langle 1\bar{1}0\rangle$, $\{111\}\langle 1\bar{1}0\rangle$ and $\{100\}\langle 011\rangle$), we simulated 2000 randomly oriented grains, and calculated the stress and strain states for each individual grain and their contribution to the elastic lattice strain. CRSS ratios between these three slip systems were tested for values of either 1 or 10 (a higher CRSS ratio indicates a stiffer slip system). A CRSS ratio of 1:10:10 for $\{110\}\langle 1\bar{1}0\rangle$, $\{111\}\langle 1\bar{1}0\rangle$ and $\{100\}\langle 011\rangle$ slip systems yields the best fit between the modelled differential elastic lattice strain ratio $\Delta\varepsilon(200)/\Delta\varepsilon(111)$ and observed ones (figure 7). This is consistent with the previous

experimental observation (Weaver and Paterson 1969, Paterson and Weaver 1970, Meade and Jeanloz 1988, Foitzik *et al* 1989) that the $\{110\}\langle 1\bar{1}0\rangle$ is the softest slip system in MgO crystals.

Acknowledgments

This research was partially supported by COMPRES, the Consortium for Materials Properties Research in Earth Sciences under NSF Cooperative Agreement EAR 01-35554. Funding was also provided by NSF grants EAR0309879, EAR0229260 and EAR0135551. Use of the National Synchrotron Light Source, Brookhaven National Laboratory, was supported by the US Department of Energy, Office of Science, Office of Basic Energy Sciences, under Contract No. DE-AC02-98CH10886. We thank Dr Z Zhong for his technical support at the X17 beam line, Dr D Lindsley for sample synthesis and Dr H Liu for his editorial support of this paper. MPI publication number 362.

References

Berveiller M and Zaoui A 1981 A simplified self-consistent scheme for the plasticity of two-phase metals *Res. Mech. Lett.* **1** 119–24

Chen J H, Li L, Weidner D and Vaughan M 2004 Deformation experiments using synchrotron x-rays: *in situ* stress and strain measurements at high pressure and temperature *Phys. Earth Planet. Inter.* **143/144** 347–56

Clausen B 1997 Characterization of polycrystal deformation by numerical modelling and neutron diffraction measurements Riso National Laboratory *Risø-R-985(EN)* Materials Research Department. Roskilde, Denmark p 85

Clausen B and Lorentzen T 1997 A self-consistent model for polycrystal deformation, description and implementation Riso National Laboratory *Risø-R-970(EN)* Roskilde, Denmark, p 42

Copley S M and Pask J A 1965a Deformation of polycrystalline MgO at elevated temperatures *J. Am. Ceram. Soc.* **48** 636–41

Copley S M and Pask J A 1965b Plastic deformation of MgO single crystals up to 1600 °C *J. Am. Ceram. Soc.* **48** 139–46

Foitzik A, Skrotzki W and Haasen P 1989 Correlation between microstructure, dislocation dissociation and plastic anisotropy in ionic crystals *Mater. Sci. Eng.* A **113** 399–407

Funamori N, Yagi T and Uchida T 1994 Deviatoric stress measurement under uniaxial compression by a powder x-ray diffraction method *J. Appl. Phys.* **75** 4327–31

Gilormini P and Bréchet Y 1999 Mechanical properties of heterogeneous media: Which material for which model? Which model for which material? *Modelling Simul. Mater. Sci. Eng.* **7** 805–16 (doi:10.1088/0965-0393/7/5/312)

Graham E K, Schwab J A, Sopkin S M and Takei H 1988 The pressure and temperature dependence of the elastic properties of single-crystal fayalite Fe_2SiO_4 *Phys. Chem. Minerals* **16** 186–98

Hearmon R F S 1956 The elastic constants of anisotropic materials–II *Adv. Phys.* **5** 323–82

Hill R 1965 Continuum micro-mechanics of elastoplastic polycrystals *J. Mech. Phys. Solids* **13** 89–101

Karato S and Wu P 1993 Rheology of the upper mantle—a synthesis *Science* **260** 771–8

Kavner A 2003 Elasticity and strength of hydrous ringwoodite at high pressure *Earth Planet. Sci. Lett.* **214** 645–54

Kavner A and Duffy T S 2001 Strength and elasticity of ringwoodite at upper mantle pressures *Geophys. Res. Lett.* **28** 2691–4

Lebensohn R A and Tome C N 1993 A self-consistent anisotropic approach for the simulation of plastic deformation and texture development of polycrystals: Application to zirconium alloys *Acta Metall. Mater.* **41** 2611–24

Li L, Weidner D, Raterron P, Chen J H and Vaughan M 2004 Stress measurements of deforming olivine at high pressure *Phys. Earth Planet. Inter.* **143/144** 357–67

Mao H-k, Shu J, Shen G, Hemley R J, Li B and Singh A K 1998 Elasticity and rheology of iron above 220 GPa and the nature of the earth's inner core *Nature* **296** 741–3

Meade C and Jeanloz R 1988 Yield strength of MgO to 40 GPa *J. Geophys. Res.* B **93** 3261–9

Merkel S, Wenk H R, Shu J, Shen G, Gillet P, Mao H-k and Hemley R J 2002 Deformation of polycrystalline MgO at pressures of the lower mantle *J. Geophys. Res.* **107** 2271 (doi:10.1029/2001JB000920)

Molinari A, Canova G R and Ahzi S 1987 A self-consistent approach of the large deformation polycrystal viscoplasticity *Acta Metall.* **35** 2983–94

Nishiyama N, Wang Y B, Uchida T, Irifune T, Rivers M L and Sutton S R 2005 Pressure and strain dependence of the strength of sintered polycrystalline Mg2SiO4 ringwoodite *Geophys. Res. Lett.* **32** (4)

Paterson M S and Weaver C W 1970 Deformation of polycrystalline MgO under pressure *J. Am. Ceram. Soc.* **53** 463–72

Reuss A 1929 Berechnung der fließgrenze von mischkristallen auf grund den konstanten des einkristalls *Z. Angew. Math. Mech.* **9** 49

Sachs G 1928 Zur ableitung einer fliessbedingung *Z. Ver. Dtsch. Ing.* **72** 734–6

Shieh S R, Duffy T S and Shen G Y 2004 Elasticity and strength of calcium silicate perovskite at lower mantle pressures *Phys. Earth Planet. Inter.* **143/144** 93–105

Singh A K 1993 The lattice strain in a specimen (cubic system) compressed nonhydrostatically in an opposed anvil device *J. Appl. Phys.* **73** 4278–86

Singh A K, Balasingh C, Mao H K, Hemley R J and Shu J 1998 Analysis of lattice strains measured under nonhydrostatic pressure *J. Appl. Phys.* **83** 7567–75

Sinogeikin S V and Bass J D 1999 Single-crystal elasticity of MgO at high pressure *Phys. Rev.* B **59** R14141–4

Sinogeikin S V, Bass J D and Katsura T 2003 Single-crystal elasticity of ringwoodite to high pressures and high temperatures: implications for 520 km seismic discontinuity *Phys. Earth Planet. Inter.* **136** 41–66

Skrotzki W and Welch P 1983 Development of texture and microstructure in extruded ionic polycrystalline aggregates *Tectonophysics* **99** 47–61

Spetzler H 1970 Equation of state of polycrystalline and single-crystal MgO to 8 kilobars and 800K *J. Geophys. Res.* **75** 2073–87

Stretton I, Heidelbach F, Mackwell S and Langenhorst F 2001 Dislocation creep of magnesiowustite $(Mg_{0.8}Fe_{0.2})O$ *Earth Planet. Sci. Lett.* **194** 229–40

Taylor G I 1938 Plastic strain in metals *J. Inst. Met.* **62** 307–15

Tingle T N, Green H W II, Young T E and Koczynski T A 1993 Improvements to Griggs-type apparatus for mechanical testing at high pressures and temperatures *Pure Appl. Geophys.* **141** 523–43

Turnock A C, Lindsley D H and Grover J E 1973 Synthesis and unit cell parameters of Ca–Mg–Fe pyroxenes *Am. Mineral.* **58** 50–9

Uchida T, Funamori N and Yagi T 1996 Lattice strains in crystals under uniaxial stress field *J. Appl. Phys.* **80** 739–46

Vaughan M T, Weidner D J, Wang Y B, Chen J H, Koleda C C and Getting I C 1998 T-cup: A new high-pressure apparatus for x-ray studies *Rev. High Pressure Sci. Technol.* **7** 1520–2

Voigt W 1928 *Lehrbuch der Kristallphysik* (Berlin: Teubner)

Wang Y B, Durham W B, Getting I C and Weidner D J 2003 The deformation-DIA: a new apparatus for high temperature triaxial deformation to pressures up to 15 GPa *Rev. Sci. Instrum.* **74** 3002–11

Weaver C W and Paterson M S 1969 Deformation of cube-oriented MgO crystals under pressure *J. Am. Ceram. Soc.* **52** 293–302

Weidner D J, Li L, Davis M and Chen J H 2004 Effect of plasticity on elastic modulus measurements *Geophys. Res. Lett.* **31** L06621 (doi:10.1029/2003GL019090)

Weidner D J, Wang Y, Chen G, Ando J and Vaughan M T 1998 Rheology measurements at high pressure and temperature *Properties of Earth and Planetary Materials at High Pressure and Temperature (Geophysical Monograph)* vol 101, pp 473–82

Wenk H-R 1999 A voyage through the deformed Earth with the self-consistent model *Modelling Simul. Mater. Sci. Eng.* **7** 699–722

Wenk R 2002 Texture and anisotropy *Plastic Deformation of Minerals and Rocks* vol 51, ed S Karato and R Wenk (Washington, DC: Mineralogical Society of America) pp 291–329

Yamazaki D and Karato S-i 2002 Fabric development in (Mg, Fe)O during large strain, shear deformation; implications for seismic anisotropy in earth's lower mantle *Phys. Earth Planet. Inter.* **131** 251–67